T1rho マッピングにおける半月板変性の評価*

中川裕介　関矢一郎　川端賢一　近藤伸平　宗田　大**

[別冊整形外科 67：36～41，2015]

はじめに

半月板は膝関節の荷重分散，衝撃吸収，安定などに寄与しており，その機能障害は関節症変化をきたす．また，中高齢者における半月板損傷は，繰り返す微小外力や加齢に伴い生じた半月板の退行変性を基盤として発生することが多いため，半月板変性の評価は重要であり，画像評価法としてMRIが大きな役割をはたしている．関節軟骨に対しては近年，質的MRIといわれる軟骨のマトリックスの変化を定量的に評価可能な撮像法が開発され，関節軟骨の評価に利用され始めている．半月板に対しても，従来のMRI以上に詳細な評価が可能となることが期待されている．本稿では質的MRIの一つであるT1rhoマッピングによる変性半月板の評価について概説するとともに，われわれの研究を紹介する．

Ⅰ．MRIによる半月板変性の評価

MRIによる半月板の評価法として，Minkの分類（grade 1：球状，不定形の高信号で半月板表面に達しないもの，grade 2：線状の高信号で半月板表面に達しないもの，grade 3A：線状の高信号で半月板表面に達しているもの，grade 3B：内部が不規則な形態の高信号で半月板表面に達しているもの）が多く用いられている．信号変化が半月板内に限局するgrade 1，2が変性で，関節内に輝度変化が連続するgrade 3が断裂と評価される[1]．しかし，実際のMRIではgrade 2と3の判別に苦慮する場合が少なくない．またMRIを用いた変形性膝関節症（膝OA）の評価方法として作成されたwhole-organ magnetic resonance imaging score（WORMS）[2,3]やBoston leeds osteoarthritis knee score（BLOKS）[4,5]では，半月板の変性評価として前者は7段階，後者は4段階に分けられ，半定量的な評価が行われている（表1）．

表1．WORMS・BLOKSにおける半月板評価（文献3，5より引用改変）

スコア	WORMS	BLOKS
0	正　常	正　常
1	実質内に限局する輝度変化	実質内に限局する輝度変化
2	小さい横断裂	単独断裂
3	単独断裂	複合断裂またはmaceration（分節化・遊離）
4	複合断裂	（－）
5	転位のある断裂	（－）
6	maceration（分節化・遊離）	（－）

Key words
MRI，T1rho mapping，meniscus degeneration

*T1rho mapping for degenerative meniscus

**Y. Nakagawa：東京医科歯科大学大学院運動器外科（Dept. of Orthop. Surg. and Sports Medicine, Graduate School of Medical and Dental Sciences, Tokyo Medical and Dental University, Tokyo）；I. Sekiya（センター長/教授）：同大学再生医療研究センター；K. Kawabata, S. Kondo, T. Muneta（教授）：同大学大学院運動器外科．

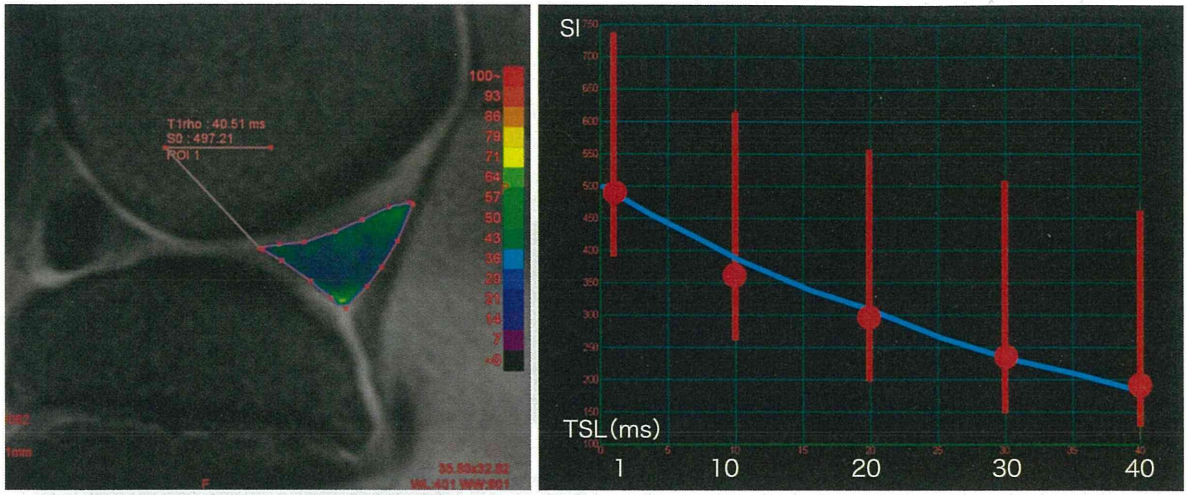

a．ザイオステーション 2 画像画面．関心領域を手動で設定すると T1rho 値が自動的に計算されカラー表示される．関心領域全体の T1rho 値が表示されるとともに，関心領域内の T1rho 値は 1 ピクセルごとにみることができる．

b．ザイオステーション 2 グラフ画面．SI：輝度，TSL：スピンロックパルス時間，赤線：関心領域中の輝度の範囲，赤点：関心領域中の輝度の平均，青線：SI（TSL）＝SI_0・exp（−TSL/T1rho）の計算式にあわせたフィッティングカーブ

図 1．T1rho マッピング解析方法

Ⅱ．質的 MRI による軟骨組織の評価

近年，MRI のハードウェア・ソフトウェア両方の進歩により T1rho マッピングや T2 マッピング，遅延相軟骨造影 MRI（dGEMRIC）などの質的 MRI が開発された．これらは軟骨のマトリックスの変化を定量的に評価することが可能なシーケンスである．その一つである T1rho マッピングは，軟骨ではグリコサミノグリカン（glycosaminoglycan：GAG）周囲に存在する水分子の動きをとらえ，軟骨中の GAG 量の変化を検出できる撮像方法である．dGEMRIC は造影剤が必要であるのに対し，T1rho マッピングではその必要がなく，より低侵襲であることが利点である．関節軟骨における基礎的な検討では，自然 OA 発症モデル動物のギニアピッグの膝関節において加齢とともに軟骨中の GAG が減少しサフラニン-O 染色性が低下すると T1rho 値が延長し，サフラニン-O 染色性と T1rho 値に負の相関を認めたことが報告されている[6]．また臨床研究で T1rho 値と X 線像による Kellgren-Lawrence（K-L）分類や MRI による WORMS と T1rho 値が相関し OA の重症度の指標となること[7]，また K-L 分類 grade 1 レベルの早期 OA の診断において T2 マッピングに比べ検出感度が高いという報告がある[8]．T1rho マッピングが関節軟骨の変性評価や，早期 OA の診断に有用であることは確立されつつある．近年，半月板変性に対しても T1rho マッピングによる評価が試みられている．Rauscher らは重度 OA の半月板の T1rho 値は軽症・中等症例より高値を示すことを報告している[9]．その他，複数の臨床研究で T1rho 値は半月板変性の評価にも有用であることが示されているが[10,11]，T1rho 値が半月板においてどのような組織変化を反映するのか，基礎的な検討は少ない．

Ⅲ．半月板における T1rho マッピングと組織所見の検討

われわれはブタ，サルを用いた動物実験において半月板における T1rho 値と組織所見の関係を検討した．

❶T1rho マッピング撮像・解析方法

3.0 T MRI（Achieva：フィリップス社，Andover）で撮像した．スピンロックパルス時間（time of spin-lock pulse：TSL）［ms］は 1，10，20，30，40 の 5 回（図 1）で撮像時間は約 15 分である．解析にはザイオステーション 2（ザイオソフト社，東京）を使用した．関心領域を手動で設定すると，フィッティングカーブが描かれ，自動的に T1rho 値が計算される．

❷マイクロミニブタを用いた半月板損傷モデルにおける検討

半月板に損傷を作成して 4 週後に，半月板の T1rho 値とコラーゲン線維構造の関連について検討した．前方から進入して内側半月板を露出し，中節に関節辺縁までい

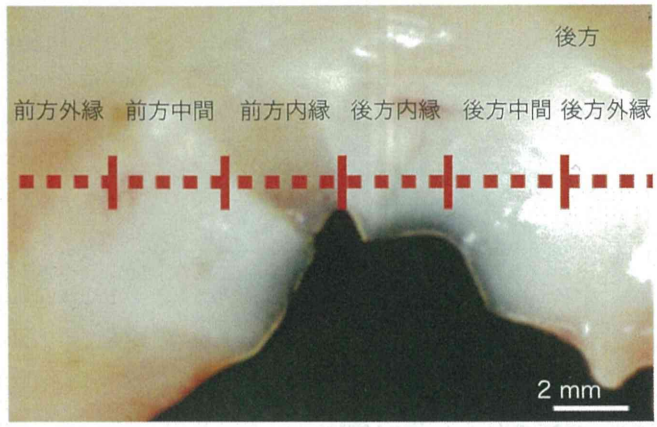

a．肉眼所見

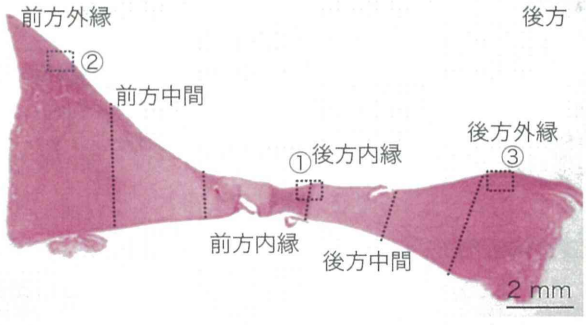

b．病理組織像（HE 染色，弱拡大）

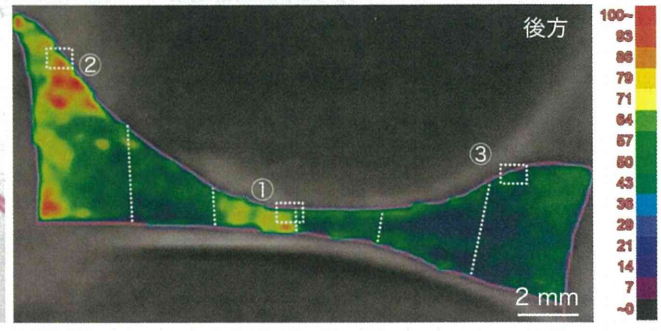

c．T1rho マッピング画像．カラースケールは 0（黒）～100 ms（赤）で表示

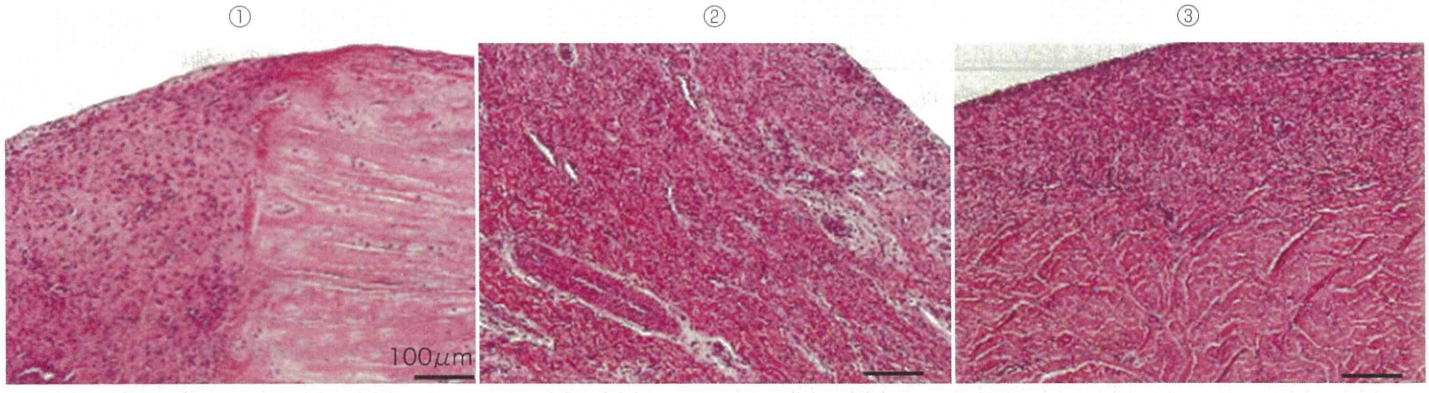

HE 染色（強拡大）

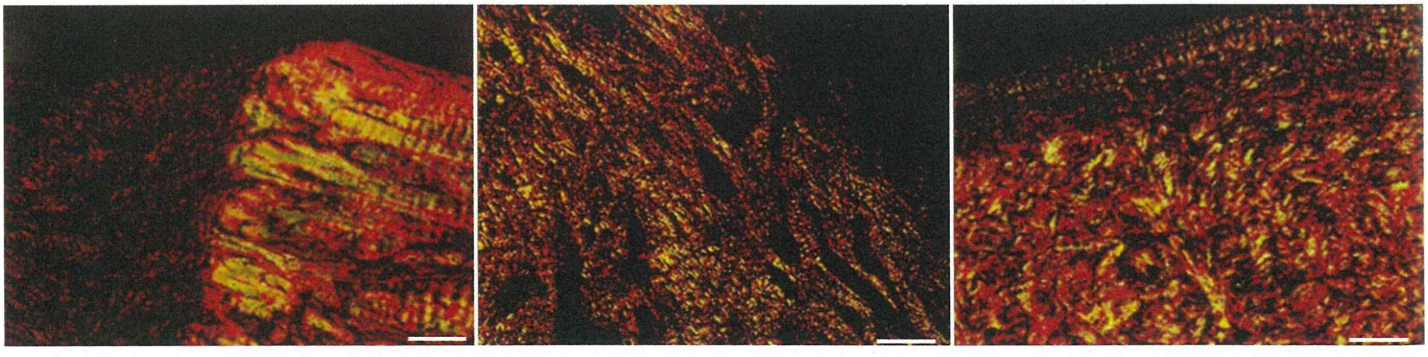

ピクロシリウスレッド染色（偏光顕微鏡で観察）

d．病理組織像［① 癒合部（前方内縁）と正常部（後方内縁）の境界，② 前方外縁，③ 後方外縁］

図 2．マイクロミニブタ半月板損傷後 4 週の所見

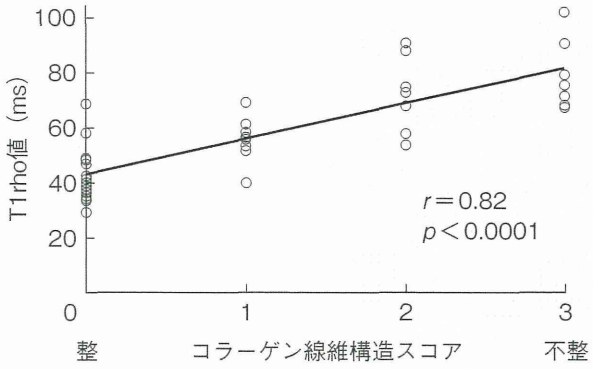

e．T1rho 値とコラーゲン線維構造スコアの相関（Spearman の順位相関係数検定）．有意な正の相関を認める．

図 2（つづき）

たる完全横断裂を作成した後，1 針縫合した．術後 4 週で肉眼的に損傷部は瘢痕組織で癒合しており，前方の外縁部は滑膜でおおわれていた（図 2a）．組織所見，T1rho マッピングを各々前・後方の内縁・中間・外縁のゾーンに分けて評価した．T1rho マッピングでは，癒合部で T1rho 値の延長を認めた（図 2b，c）．① で示す前方内縁の癒合部と後方内縁との境界は T1rho 値の違いが明瞭である．T1rho が延長している癒合部の組織所見は HE 染色で新生血管が観察され（図 2d），ピクロシリウスレッド染色による偏光顕微鏡の観察で，輝度は非常に低く，コラーゲン線維構造が未熟である．②，③ は前・後方の外縁であるが，前方外縁の T1rho 値は後方に比べ延長している．組織学的に ② は滑膜炎により表層部は肥厚し，滑膜組織の浸潤で多数の血管形成を認め，コラーゲン線維間に多数の細胞が浸潤し構造は不整となっている．また，偏光顕微鏡では輝度が低下している．③ は表層部に軽度の滑膜様細胞を認め，表層は肥厚しているが実質部は正常の線維構造が保たれている．コラーゲン線維構造を 0（正常）～3（重度の不整化/線維構造なし）の 4 段階のスコアで評価し，T1rho 値との関連を検討すると有意な正の相関を認めた（図 2e）．コラーゲン線維構造が不整になると T1rho 値が延長することが示された．

❸サルを用いた加齢性変性半月板モデルにおける検討

加齢による変性変化が予想される高齢のサル半月板における T1rho 値とサフラニン-O 染色性の関連性を検討した．カニクイサルの寿命は 15 年程度であるが，12～13 歳の外側半月板を用いた．肉眼的に半月板は黄色不透明であり，断裂所見は認めなかった（図 3a）．組織学的に変性所見である空胞化（軟骨細胞の細胞死を反映）が存在した（図 3b）．内縁・中間ゾーンのサフラニン-O 染色性が低下している半月板で，T1rho 値が延長していた．サフラニン-O 染色性を 0（なし）～3（強）の 4 段階のスコアで評価し，T1rho 値との関連を検討した．無血行野で線維軟骨領域である内縁・中間のゾーンでは T1rho 値とスコアに有意な負の相関を認めた（図 3c）．サフラニン-O 染色性が低下すると T1rho 値が延長することが示された．

Ⅳ．T1rho マッピングによる半月板変性の評価

OA 患者の内側半月板後節の T1rho 値は，断裂がある症例では断裂がない症例に比べ延長していたことが報告されている[11]．本検討で T1rho 値はコラーゲン構造の不整化の程度と正の相関を示し，T1rho マッピングは変性断裂の評価に有用であると考えられた．また Mink 分類 grade 2 など，断裂にいたらない半月板内部の輝度変化はムコイド変性によるものと考えられている．ムコイド変性はコラーゲン線維構造の乱れや水分含有量の上昇を伴うことから，T1rho 値は延長すると考えられる．われわれの高齢サルにおける検討では，T1rho マッピングは半月板において GAG 量（サフラニン-O 染色性）の変化を反映することが明らかとなった．線維軟骨組織である半月板に含まれる GAG 量は硝子軟骨組織の関節軟骨の約 1/6 とされ，半月板において含有量が少ない GAG 量の変化を T1rho マッピングが反映できるかはこれまで不明であった．半月板は組織構造や生化学的組成が部位により異なり，内縁は無血行野で GAG 量が高くコラーゲン量が少ない硝子軟骨に近い組織であり，外縁は血行野で GAG 量が低くコラーゲン量が多い線維性組織である[12]．半月板をゾーンに分け評価することで，GAG 濃度が相対的に高い内縁と中間ゾーンでは GAG 量の変化が検出可能となったと考えられる．近年の報告で，Son らは人工

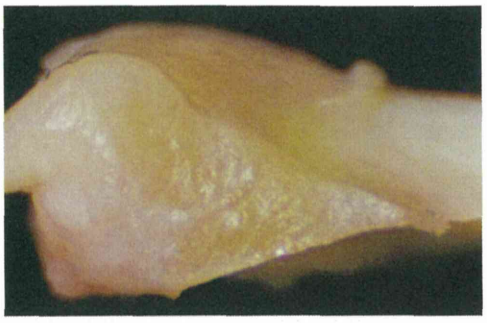

a．肉眼所見．矢状断での切離面を示す．

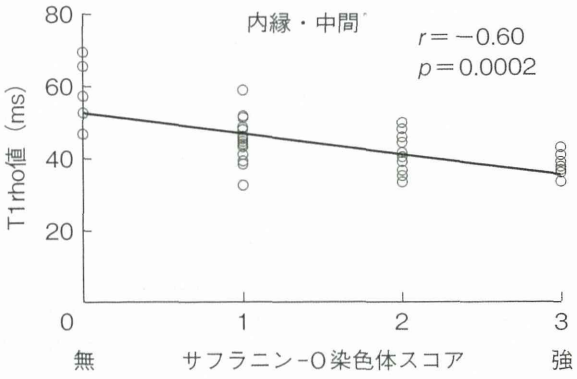

c．T1rho 値とサフラニン-O 染色性スコアの相関（Spearman の順位相関係数検定）．有意な負の相関を認める．

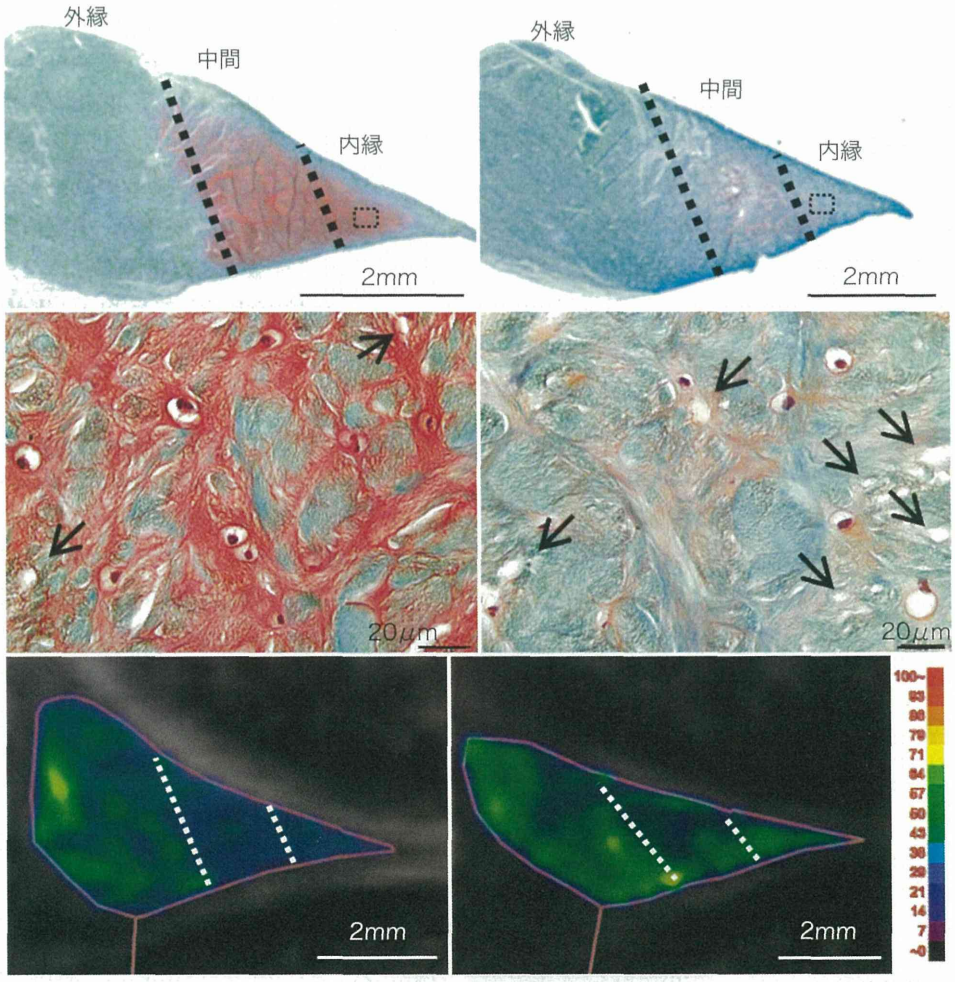

b．右段：変性が強い半月板，左段：変性が弱い半月板，上段：サフラニン-O 染色（弱拡大），中段：内縁のサフラニン-O 染色（強拡大）［矢印：empty lacuna］，下段：T1rho マッピング画像．カラースケールは 0（黒）～100 ms（赤）で表示

図 3．高齢サル半月板

膝関節全置換術患者の摘出した半月板を同様に内縁，中間，外縁に分け，T1rho 値と GAG 量の関係を検討したところ，内縁の GAG 量が中間より有意に低く，T1rho 値も中間より有意に延長したことを報告している[13]．Pauli らは，ヒト死体膝の検討で変性変化は内・外側半月板とも内縁から起こることを報告している[14]．われわれも検討したように，部位ごとに関心領域を設定しマッピングを行うことを zonal mapping という．関節軟骨においては表層，深層の 2 層に分ける zonal mapping で，表層から進行する前十字靱帯再建術後の早期軟骨変性が検出可能とな

ることが報告されている[15]．半月板においてもGAG量の変化を評価できるT1rhoマッピングでzonal mappingを行うことは内縁から始まる早期の変性評価を検出でき，早期の半月板変性の評価に有用であると考えられる．そのためには半月板各部位ごとのT1rho値の正常値の検討や，zonal mappingを半自動的に行えるようなソフトウェアの開発が望まれる．

ま と め

T1rhoマッピングは半月板においてコラーゲン，GAG量の変化を反映し，質的な評価が可能であるため，半月板変性の評価に有用である．評価の際には半月板の部位による組織・生化学的組成の差を考慮して評価する必要がある．

文 献

1) Mink JH, Deutsch AL：Magnetic resonance imaging of the knee. Clin Orthop **244**：29-47, 1989
2) Peterfy CG, Guermazi A, Zaim S et al：Whole-organ magnetic resonance imaging score（WORMS）of the knee in osteoarthritis. Osteoarthritis Cartilage **12**：177-190, 2004
3) Wang L, Chang G, Xu J et al：T1rho MRI of menisci and cartilage in patients with osteoarthritis at 3T. Eur J Radiol **81**：2329-2336, 2012
4) Hunter DJ, Lo GH, Gale D et al：The reliability of a new scoring system for knee osteoarthritis MRI and the validity of bone marrow lesion assessment：BLOKS（Boston leeds osteoarthritis knee score）. Ann Rheum Dis **67**：206-211, 2008
5) Crema MD, Hunter DJ, Roemer FW et al：The relationship between prevalent medial meniscal intrasubstance signal changes and incident medial meniscal tears in women over a 1-year period assessed with 3.0 T MRI. Skeletal Radiol **40**：1017-1023, 2011
6) Fenty MC, Dodge GR, Kassey VB et al：Quantitative cartilage degeneration associated with spontaneous osteoarthritis in a guinea pig model. J Magn Reson Imaging **35**：891-898, 2012
7) Regatte RR, Akella SV, Wheaton AJ et al：3 D-T1rho-relaxation mapping of articular cartilage；*in vivo* assessment of early degenerative changes in symptomatic osteoarthritic subjects. Acad Radiol **11**：741-749, 2004
8) Li X, Benjamin Ma C, Link TM et al：*In vivo* T（1rho）and T（2）mapping of articular cartilage in osteoarthritis of the knee using 3T MRI. Osteoarthritis Cartilage **15**：789-797, 2007
9) Rauscher I, Stahl R, Cheng J et al：Meniscal measurements of T1rho and T2 at MR imaging in healthy subjects and patients with osteoarthritis. Radiology **249**：591-600, 2008
10) Wang L, Chang G, Bencardino J et al：T1rho MRI of menisci in patients with osteoarthritis at 3 Tesla；a preliminary study. J Magn Reson Imaging **40**：588-595, 2014
11) Zarins ZA, Bolbos RI, Pialat JB et al：Cartilage and meniscus assessment using T1rho and T2 measurements in healthy subjects and patients with osteoarthritis. Osteoarthritis Cartilage **18**：1408-1416, 2010
12) Nakano T, Dodd CM, Scott PG：Glycosaminoglycans and proteoglycans from different zones of the porcine knee meniscus. J Orthop Res **15**：213-220, 1997
13) Son M, Goodman SB, Chen W et al：Regional variation in T1rho and T2 times in osteoarthritic human menisci；correlation with mechanical properties and matrix composition. Osteoarthritis Cartilage **21**：796-805, 2013
14) Pauli C, Grogan SP, Patil S et al：Macroscopic and histopathologic analysis of human knee menisci in aging and osteoarthritis. Osteoarthritis Cartilage **19**：1132-1141, 2011
15) Li X, Kuo D, Theologis A et al：Cartilage in anterior cruciate ligament-reconstructed knees；MR imaging T1rho and T2 initial experience with 1-year follow-up. Radiology **258**：505-514, 2011

* * *

Original Article

High capacity of purified mesenchymal stem cells for cartilage regeneration

Eriko Grace Suto[1,], Yo Mabuchi[1,**], Nobuharu Suzuki[1)], Asuka Koyanagi[1)], Yoshiko Kawabata[1)], Yusuke Ogata[1)], Nobutake Ozeki[2)], Yusuke Nakagawa[2)], Takeshi Muneta[2)], Ichiro Sekiya[3)] and Chihiro Akazawa[1,*)]**

[1)]Department of Biochemistry and Biophysics, Graduate School of Health Care Sciences, Tokyo Medical and Dental University, Bunkyo-ku, Tokyo, Japan
[2)]Department of Joint Surgery and Sports Medicine, Tokyo Medical and Dental University, Bunkyo-ku, Tokyo, Japan
[3)]Department of Applied Regenerative Medicine, Tokyo Medical and Dental University, Bunkyo-ku, Tokyo, Japan

Mesenchymal stem cells (MSCs) are a heterogeneous population of cells that proliferate and differentiate into bone, cartilage, and fat *in vitro*. Because of this multi-potency, the therapeutic applications of MSCs are under intensive exploration. The most common and redundant method for MSC cultivation requires prolonged culture on plastic dishes. The current study compared the differentiation/proliferative potency of purified mouse MSCs (CD45$^-$/ TER119$^-$/PDGFRα$^+$/ Sca-1$^+$ cells, or PαS cells) with whole bone marrow (WBM)-derived, plastic-adherent MSCs. After three passages, the surface expression levels of CD45, TER119, PDGFRα, and Sca-1 were evaluated in WBM and PαS cells. While PαS cells maintained high expression levels of both PDGFRα and Sca-1, WBM cells exhibited less expressed levels of these stem cell makers. Additionally, WBM cell cultures were frequently contaminated by CD45$^+$ hematopoietic cells. Both cell migration and proliferation were significantly higher in PαS vs. WBM cells, indicating the enhanced differentiation potential of PαS cells for the mesenchymal lineage, and suggesting that WBM cell heterogeneity may regulate and limit the stemness of their MSC progeny. Consistent with this hypothesis, PαS cells transplanted locally at sites of cartilage defects displayed higher cartilage regeneration capacity than WBM cells in a rat osteochondral defect model. This is the first report to demonstrate its improved contribution to cartilage repair *in vivo*. Thus, the protocol employed for MSC isolation is crucial for the effective translation of MSC multi-potency into clinical therapeutics.

Rec.9/29/2014, Acc.1/6/2015, pp78-85

*Correspondence should be addressed to:
Chihiro Akazawa, Professor, Department of Biochemistry and Biophysics, Graduate School of Health Care Sciences, Tokyo Medical and Dental University, Bunkyo-ku, Tokyo 113-8510, Japan. Phone: +81-3-5803-5364; E-mail: c.akazawa.bb@tmd.ac.jp

**These authors contributed equally to this work.

Key words bone marrow, cartilage, mesenchymal stem cell, regeneration, stem cell therapy

Introduction

The clinical treatment of cartilage injury is still challenging for orthopedic surgeons, because cartilage shows a weak competency for self-repair. Bone marrow (BM) contains both hematopoietic stem cells and non-hematopoietic mesenchymal stem cells (MSCs). These BM-derived MSCs can be isolated from the adult BM, expanded *in vitro*, and differentiated into several types of specialized cells, including osteocytes, chondrocytes, and adipocytes[1]. The most commonly used isolation technique for MSCs requires a prolonged period of culture on plastic dishes. However, MSCs expanded in this manner gradually undergo differentiation, exhibiting altered morphological features and functions from the parent stem cells. The differentiation process alters the nature of immature MSCs, making it difficult to identify and study their *in vivo* functional characteristics. Currently, several clinical studies have been performed with MSCs without even understanding their role in tissue regeneration.

Articular cartilage covers the ends of the bone and provides a flexible connective tissue, and is composed of extracellular matrix molecules, ground substance, and chondrocytes[2]. Osteoarthritis occurs following the loss of articular cartilage, leading to boney injury with pain, stiffness, and loss of movement[3]. Osteoarthritis is the most common cause of arthritis worldwide and engenders a significant burden on health care budgets[4]. Due to the avascular nature of cartilage, there is little hope for spontaneous self-repair, and joint replacement is therefore a major option for osteoarthritis patients.

In vivo studies using rabbits and mice demonstrated that MSC aggregates can promptly adhere to osteochondral defects and thereafter promote the regeneration of cartilage[5, 6]. This methodology may theoretically be incorporated into a medical treatment for osteoarthritis patients. MSCs hold significant promise for cartilage repair, and various ongoing trials are investigating their ability to improve osteoarthritis outcomes. Intuitively, it is important to isolate the most potent subpopulation of MSCs for use in regenerative strategies, including those intended for cartilage repair. Although cells isolated by the plastic-adherence protocol lose much of their stemness, prospectively-isolated, purified mouse MSCs (i.e., cluster of differentiation 45 (CD45)$^-$/erythroid cell marker, Ly76 (TER119)$^-$/platelet-derived growth factor receptor α (PDGFRα)$^+$/stem cell antigen-1 (Sca-1)$^+$ cells, or PαS cells) have recently garnered attention due to their significantly enhanced colony-forming unit-fibroblast (CFU-F) ability[7, 8]. PαS cells also differentiate more efficiently into adipocytes, osteocytes, and chondrocytes relative to PDGFRα$^+$ or Sca-1$^+$ single-positive cells *in vitro*. Given the large number of researchers performing mouse MSC investigations by using PαS cells, PDGFRα and Sca-1 are becoming the standard markers for the identification of MSCs, especially when they are co-expressed[9-11]. However, it still remains unexplained the regenerative effects of the PaS cells on tissue defect model.

The application of MSCs to cartilage regeneration is one of the more advanced fields in MSCs clinical study. In the present study for the first time, we compared the differentiation and proliferative potency of mouse PαS cells with whole BM (WBM)-derived MSCs *in vitro*. We then separately transplanted the mouse PαS and WBM cells into an osteochondral defect in rats and monitored the chondrogenic differentiation of the cells *in vivo*. Our results indicate that purified MSCs have enhanced therapeutic potential for cartilage repair. This protocol employed for MSC isolation is crucial for the effective translation of MSC multi-potency into clinical therapeutics.

Materials and methods

1)Animals

Adult C57BL/6-Tg (cytomegalovirus enhancer (CAG)-enhanced green fluorescent protein (EGFP)) mice at 6-8 weeks of age were purchased from Japan SLC, Inc. (Shizuoka, Japan). LEW/CrlCrlj rats at 10-12 weeks of age were purchased from Japan Charles River (Yokohama, Japan). Animal care was in strict accordance with the guidelines of the Animal Care and Use Committee of Tokyo Medical and Dental University (Tokyo, Japan).

2)Isolation and culture of mouse MSCs

Femurs, tibias, and ilia were dissected from mice and crushed with a muddler. The fragments were gently washed once in HBSS+ solution containing 2% fetal bovine serum (FBS; HyClone Laboratories, Logan, UT, USA), 10 mM HEPES (Wako Pure Chemicals, Ltd., Osaka, Japan), and 1% penicillin/streptomycin (Gibco BRL, Grand Island, NY, USA). The washed fragments were filtered through a Falcon™ 70-μm cell strainer (BD, Franklin Lakes, NJ, USA), and the filtrate was discarded. The bone fragments were collected into Dulbecco's modified Eagle's medium (DMEM; Life Technologies, Grand Island, NY, USA) containing 0.2% collagenase (Wako), 10 mM HEPES, 1% penicillin/streptomycin, and 25 U/mL DNase1 (Sigma

Chemical Co., St. Louis, MO, USA). The mixture was incubated for 1 h at 37°C with shaking. The suspension was filtered through a 70-μm cell strainer to remove the bone fragments and centrifuged at 280 × g for 7 min. The pellet was mechanically disrupted, and sterile water (1 mL) was added for 6 sec. Next, 2× phosphate buffered saline (PBS) containing 4% FBS was added, and the mixture was filtered through a 70-μm cell strainer and centrifuged at 280 × g for 7 min. The pellet was then used for antibody staining, as described below.

For antibody-mediated isolation of PαS cells, the cell pellet was diluted in HBSS+ and stained for 30 min on ice with the following mouse primary antibodies: anti-phycoerythrin (PE)-conjugated Sca-1 and anti-PE-conjugated CD31, anti-PE-Cy7-conjugated CD45, anti-PE-Cy7-conjugated TER119, and anti-allophycocyanin (APC)-conjugated PDGFRα (eBioscience, San Diego, CA, USA). For cell surface marker analysis, we used anti-PE-conjugated CD31. Flow cytometry and cell sorting were performed by using a MoFlo instrument (Beckman Coulter, Miami, FL, USA). Propidium iodide (PI) fluorescence was used for gating dead cells. Sorted cells were plated at a density of 3000 cells per dish in non-coated 10-cm culture dishes and incubated at 37°C in MSC media containing DMEM-GulutaMAX (Life Technologies), 20% FBS, 20 ng/mL basic fibroblast growth factor (ReproCELL, Kanagawa, Japan), and 1% penicillin/streptomycin.

3)Multi-lineage differentiation of WBM and PαS cells

For adipogenic induction, 1.0×10^4 cells at passage 3 were plated into 24-well plates with adipogenic induction media (Lonza, Walkersville, MD, USA) and incubated at 37°C in an atmosphere containing 5% humidified CO_2. For osteogenic induction, 0.7×10^4 cells at passage 3 were plated into 24-well plates with osteogenic induction media (Lonza) and incubated at 37°C with 5% humidified CO_2. Both adipogenically- and osteogenically-differentiated cells were cultured for 2 weeks. For the chondrogenesis assay, 5.0×10^5 cells at passage 3 were placed into a 15-mL polypropylene tube (Nalge Nunc International, Rochester, NY, USA) and centrifuged at 200 × g for 4 min. The pellet was cultured in chondrogenic induction media (Lonza) containing 500 ng/mL bone morphogenic protein (BMP) 6 plus 10 ng/mL transforming growth factor beta 3 (TGFβ3; R&D Systems, Minneapolis, MN, USA) and incubated at 37°C with 5% humidified CO_2 for 4 weeks.

4)Quantitative analysis of *in vitro* cell differentiation

Adipogenically-differentiated cells were stained with Oil red O (Muto Pure Chemicals Co., Ltd., Tokyo, Japan) and extracted by using 2-propanol (Wako). The absorbance at 510 nm was then measured. Osteogenically-differentiated cells were stained with alizarin red (Millipore, Billerica, MA, USA) and extracted by using 10% acetic acid. The absorbance at 405 nm was then determined. Chondrogenically-differentiated cell pellets were embedded in paraffin and cut into 4-μm-thick sections. The paraffin-embedded sections were then double-stained with primary mouse anti-chick collagen 2 (Col2) antibody (Developmental Studies Hybridoma Bank, Iowa City, IA, USA) and 4',6-diamidino-2-phenylindole (DAPI).

5)Immunofluorescence staining

The anti-Col2 antibody was employed for immuno-fluorescence staining of MSC aggregates. After fixation in 4% paraformaldehyde (Wako), cells on slides were treated with hyaluronidase for 1 h at 37°C and blocked with Blocking One solution (Nacalai Tesque, Kyoto, Japan) for 30 min at room temperature. Next, the slides were incubated with primary antibody at a 1:100 dilution in 2 mg/ml hyaluronidase solution overnight at 4°C, followed by an Alexa Fluor-conjugated anti-mouse immunoglobulin G (IgG) (Invitrogen, Carlsbad, CA, USA) at a 1:500 dilution for 30 min at room temperature. Slides were mounted with Vector shield (Vector Laboratories, Burlingame, CA, USA) containing DAPI and examined on a Leica TCS-SP5 confocal laser scanning microscope (Leica Microsystems, Biberach, Germany).

6)Migration assay

To analyze the proliferative potential of MSC donor cells, MSC aggregates were plated into 24-well plates, and colony size was measured each day. Cell division was analyzed by staining with an antibody against Ki67 (BD), a marker of cell proliferation.

7)MSC transplantation into rats

Mouse MSCs at passage 3 were cultured in hanging drops (25×10^4 cells/drop) with MSC media and cultured for 3 days at 37°C with 5% humidified CO_2. Under isoflurane anesthesia, the rat knee joint was incised, and the patella was dislocated. An osteochondral defect (1.8 mm in diameter) was created in the medial condyle of the femur. Four MSC aggregates (100×10^4 cells) were inserted into

Table 1 Primer sequences for quantitative RT-PCR

Target		Sequence
HPRT	Forward	5' TCAGTCAACGGGGGACATAAA 3'
	Reverse	5' GGGGCTGTACTGCTTAACCAG 3'
TGFb3	Forward	5' CCCTGGACACCAATTACTGC 3'
	Reverse	5' TCAATATAAAGGGGGCGTACA 3'
BMP6	Forward	5' AACCGGTCCACCCAGTCGCA 3'
	Reverse	5' TCCATcACAGTAGTTGGCAGC 3'
MMP13	Forward	5' CAGTCTCCGAGGAGAAACTATGA 3'
	Reverse	5' GGACTTTGTCAAAAAGAGCTCAG 3'

the defect. The defect was left empty in control animals. The patella was then relocated, and the wound was closed. Rats were sacrificed at 4 or 8 weeks after the operation.

8)Histological examination

The dissected femurs were immediately embedded in Super Cryo Embedding Medium (Section-lab, Co., Ltd., Hiroshima, Japan) and frozen with dry ice and hexane. The tissue block was cut into 12-μm-thick sections, fixed in a 4% paraformaldehyde solution, and washed in PBS. The frozen sections were stained 1 with anti-Col2 antibody.

9)RT-PCR

Total RNA was prepared with TRI reagent (Sigma-Aldrich). The quantitative RT-PCR was performed using the StepOne real-time PCR system (Life Technologies). cDNA was amplified with 50 PCR cycles at 95°C for 3 seconds, 60°C for 30 seconds using FAST SYBR Green Master Mix (Life Technologies) and gene-specific primers (Table 1).

10)Statistical analysis

Quantitative data are presented as the means ± the standard deviation (SD) from at least 3 representative experiments. For statistical analysis, the data were evaluated with Student's *t*-test. In all cases, *p*-values of < 0.05 were considered significant.

Results

1)Isolation and characterization of WBM and PαS cells

Mouse WBM was stained with antibodies against the following antigens: CD45, Ter119, PDGFRα, and Sca-1. Flow cytometry analysis demonstrated the presence of PDGFRα and Sca-1 in a subpopulation of cells and allowed the isolation of PDGFRα$^+$Sca-1$^+$ PαS cells and all living

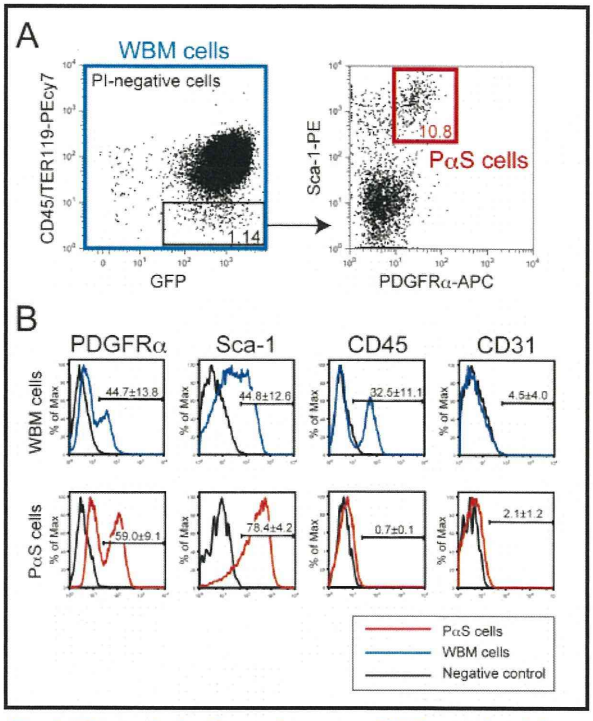

Fig.1 Characterization of mouse MSCs derived from WBM cells and the prospectively-isolated PDGFRα$^+$Sca-1$^+$ cell fraction

(A) Representative flow cytometric profiles of the PI-negative WBM cell population (WBM: blue gated) and the CD45$^-$Terr119$^-$ PDGFRα$^+$Sca-1$^+$ cell population (PαS: red gated) derived from CAG-EGFP mice. Numbers adjacent to the outlined areas indicate the percentage of gated cells in total WBM mononuclear cells.

(B) Surface marker expression in WBM and PαS cells after three passages. Unlabeled cells (negative control) are included for comparison. Numbers indicate the means ± the SEM.

PI$^-$ (WBM) cells (Fig. 1A). Analysis of surface marker in both populations in culture (passage 3) demonstrated that PαS maintain expression of PDGFRα and Sca-1 makers in contrast to WBM cells (Fig. 1B). Cultured WBM-MSCs contained a substantial percentage of contaminating CD45$^+$ hematopoietic cells (32.5 ± 11.1%).

2)Multi-lineage potential differences between WBM and PαS cells

After three passages, PαS and WBM cells were transferred into an adipogenic induction medium. Both cell types adopted a rounded shape and showed evidence of lipid vesicle formation after 14 days in differentiation medium and staining with Oil red O (Fig. 2A). Adipocyte generation was quantitatively analyzed via absorption spectrometry analysis